CONTEMP. PHYS. 1980, VOL. 21, NO. 3, 219–242

Silicon–Germanium Alloys as High-Temperature Thermoelectric Materials

C. M. BHANDARI† and D. M. ROWE

University of Wales Institute of Science and Technology, Cardiff

ABSTRACT. This article reviews the preparation and properties of silicon–germanium alloys, mentions some recent developments in their technology, and assesses their potential for further improvement as high temperature thermoelectric materials.

1. Introduction

Although the direct conversion of heat into electrical energy by the thermoelectric effect has been known for perhaps a century, it was not until the advent of the transistor and the subsequent extensive research into compound semiconductors that there emerged materials suitable for the development of thermoelectric generators as practical sources of electrical energy.

The American Space programmes of the late 1950s and early 1960s required reliable and durable sources of electrical energy for space vehicles and satellites. Thermoelectric generators are ideally suited to such applications. Further, they have found many other uses in medical, terrestrial and marine applications, where their desirable properties outweigh the relatively high cost and low conversion efficiency, which is typically about 5%.

The conversion efficiency of a generator depends upon the properties of its thermocouple materials as expressed by a 'figure of merit', Z, which itself depends on the electrical and thermal properties. Three technologies can be described as established, those based upon (*a*) bismuth telluride, (*b*) lead telluride and (*c*) silicon–germanium alloys. The upper operating temperatures range from around 250°C for bismuth telluride Bi_2Te_3 and 500°C for lead telluride PbTe, to 1000°C for silicon-germanium alloys referred to generally as silicon–germanium, Si–Ge, and specifically by composition e.g. 0·78 Si–0·22 Ge (meaning atomic proportions) (fig. 1). Silicon–germanium alloys are among the best high temperature materials.

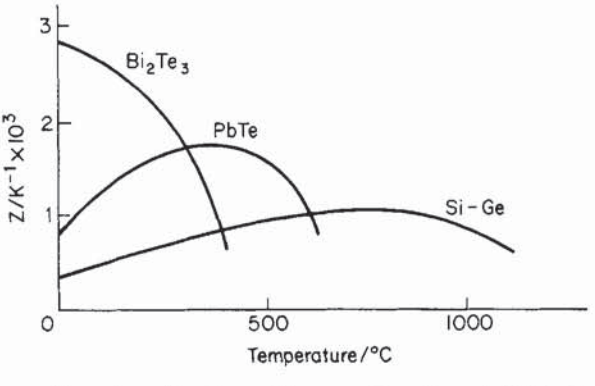

Fig. 1. Figure of merit as function of temperature for established materials.

† Present address: University of Allahabad, India.

0010-7514/80/2103 0219 802·00

The conversion efficiency is given approximately as $\frac{1}{4}Z\Delta T$ where ΔT is the temperature difference between hot and cold junctions. So although the figures of merit of the three materials differ substantially, with silicon–germanium the lowest, their performance is comparable when each is being used over the extreme of its operating temperature range. However, the conversion efficiency is not the only consideration. When we select a material for a specific application, other factors such as the direct output voltage, thermal losses and also the reliability must be taken into acount.

Thermoelectric generators conventionally provide relatively high currents and low voltages. Most applications require something of the order of a few volts and for high power levels this can be done by having sufficient numbers of thermocouples in series. At low power levels miniaturization of a conventional thermocouple configuration reduces the output voltage, which if we step up with a d.c.–to–d.c. converter decreases the overall efficiency. Thermoelements of silicon–germanium can be made with large length : cross-section ratios leading to low power levels at relatively high voltages with reasonable conversion efficiency.

Significant developments have also been made in a new group of thermoelectric semiconductors, the selenides. Recently, it has been shown that the figure of merit can be improved by using fine grained alloys rather than single crystal material. This is because of the lowering of thermal conductivity due to the scattering of phonons at grain boundaries; a phenomenon which favours materials such as silicon–germanium alloys whose constituent elements have atoms differing considerably in mass.

2. Basic concepts and thermoelectric phenomena

The basic concepts of thermoelectricity have been described in a previous issue of *Contemporary Physics* (Bateman 1960) and need only be dealt with briefly here.

When a steady temperature gradient is maintained along a conductor, the free electric charge carriers at the hot end will tend to diffuse towards the cold end. The temperature gradient thus also leads to a potential gradient along the conductor. If a complete circuit formed from two dissimilar conductors a and b with associated Seebeck coefficients α_a and α_b which are electrically in series, but thermally in parallel as fig. 2, the open-circuit-voltage (e.m.f.) developed is $V_{ab}=(\alpha_a-\alpha_b)\ (T_H-T_C)$. For small temperature differences the energy used to transport the electric charge carriers along the temperature gradient can be neglected. This

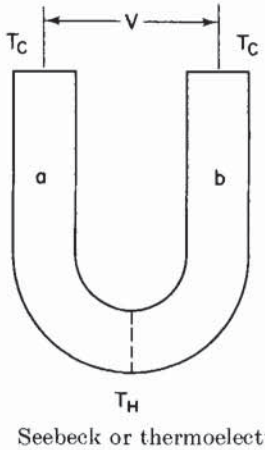

Fig. 2. Seebeck or thermoelectric effect.

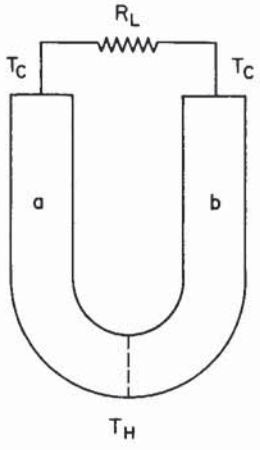

Fig. 3. Schematic thermoelectric generator.

relationship is then linear with temperature and defines the Seebeck coefficient of the junction. If now a load resistance R_L is connected across the cold end of the thermocouple arrangement (fig. 3) heat will be absorbed at the hot junction, some will be rejected at the cold junction and the rest will drive a current through the circuit and deliver power to the load.

The efficiency of such a generator is the ratio of the energy supplied to the load to the energy absorbed as heat at the hot junction (or correspondingly in terms of power). It depends on the ratio of the load resistance to the generator's internal resistance and at maximum power it can be shown that the efficiency is

$$(T_H - T_C)\left(\frac{3T_H}{2} + \frac{T_C}{2} + \frac{4}{Z}\right)$$

while the maximum efficiency is $\varepsilon\gamma$ where

$$\varepsilon = \frac{T_H - T_C}{T_H}, \quad \gamma = \frac{(1+Z_c\bar{T})^{1/2} - 1}{(1+Z_c\bar{T})^{1/2} + T_C/T_H}, \quad \text{and} \quad \bar{T} = \frac{T_H + T_C}{2}.$$

Here Z_c is the figure of merit of the junction defined as $(\alpha_c)^2/Rk'$ where α_c is the Seebeck coefficient of the junction, k' the thermal conductance of a and b in parallel, and R the electrical resistance of a and b in series. (The units for Z_c work out to K^{-1}; the product Z_cT is thus dimensionless and can be called the dimensionless figure of merit). If the geometrics of a and b are arranged to minimize heat absorption, then

$$\frac{R_a}{R_b} = \left(\frac{\rho_a k_a}{\rho_b k_b}\right)^{1/2}$$

and

$$Z_c = (\alpha_a - \alpha_b)^2 \Big/ \left[\left(\frac{k_a}{\sigma_a}\right)^{1/2} + \left(\frac{k_b}{\sigma_b}\right)^{1/2}\right]^2$$

Here $\sigma = 1/\rho$ and k are the electrical and thermal conductivities.
In practice the two arms of the junction are similar materials as to the values of k and σ, and can be considered as a single material whose figure of merit is given by

$$Z = \frac{\alpha^2\sigma}{k}$$

The thermal conductivity k is the sum of a contribution k_L arising from lattice waves and a contribution k_e from the charge carriers. In actual devices a large number 'N' of couples are connected electrically in series to form a 'module' which is subject to heat losses. Under matched load conditions when maximum power is so transferred to the load the module efficiency is given by

$$\frac{\frac{1}{2}\varepsilon}{\left(1-\frac{1}{4}\varepsilon+\frac{2}{ZT_H}\right)}\left(1-\frac{Q_s}{Q}\right),$$

where

$$Q=Q_m+Q_s.$$

Here $Q_m=2Nmk\Delta T\,(1+\frac{1}{2}ZT_H\,(1-\frac{1}{4}\varepsilon)$ is the heat extracted by the module of N couples with p- and n- type arms each of thermal conductivity k and area-to-length ratio m and Q_s is the heat loss by other means. ΔT is the temperature difference across the module.

All these parameters occuring in the figure of merit depend on the carrier concentration (which can be expressed in terms of the Fermi energy ξ where $\xi=0$ corresponds to $\sim 10^{25}\,m^{-3}$ and $\xi=2$ to about $10^{26}\,m^{-3}$, and the expected dependence of α, σ and k are as shown in fig. 4. The figure of merit has a maximum at a carrier concentration of around $10^{25}\,m^{-3}$—which means, in heavily doped semiconductors.

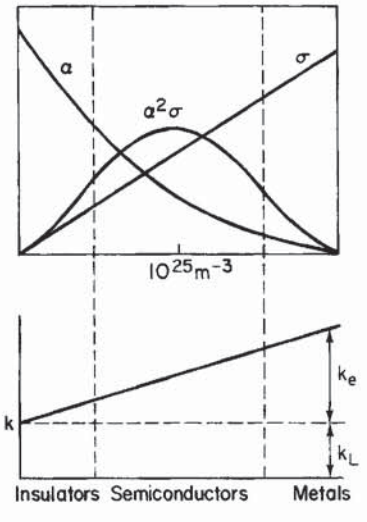

Fig. 4. Dependence of α, σ and k on concentration of free carriers.

3. Thermoelements and silicon–germanium generators

Thermoelectric generators are essentially low voltage devices and even for such use, since the Seebeck coefficients are about $200\,\mu VK^{-1}$, a number of thermocouples must be connected electrically in series and hence thermally in parallel. This means many contacts, with the consequent difficulties, which are worst at high temperatures.

Neither gold nor aluminium is suitable for high temperature contacts because both form low melting point eutectics with silicon–germanium, while a material which diffuses readily such as nickel affects the thermoelectric properties of the

thermoelements. Tungsten is suitable as an intermediary material to silicon–germanium up to about 700°C but above this temperature it reacts chemically and also presents other problems.

The more refractory the material, the more difficult it is to make good electrical contacts. The expansivity of Si–Ge is very low so it is difficult to make reliable and durable low resistivity contacts with it. Tungsten is useless in an oxidising atmosphere. Low temperature contacts to Si–Ge can be made by electroplating gold on to the prepared surface, followed by gold sputtering and pressure baking. The temperature of operation is again restricted to something less than 500°C by the formation of eutectics. Attempts are being made to extend the temperature of operation by r.f. sputtering of multilayer films using molybdenum as an intermediary. High temperature contacts to Si–Ge alloys have been made with niobium and molybdenum. Niobium can be spot-welded to Si–Ge and molybdenum soldered using a suitably doped tin solder. Pressure contacts using heavily doped slices of silicon have also been employed.

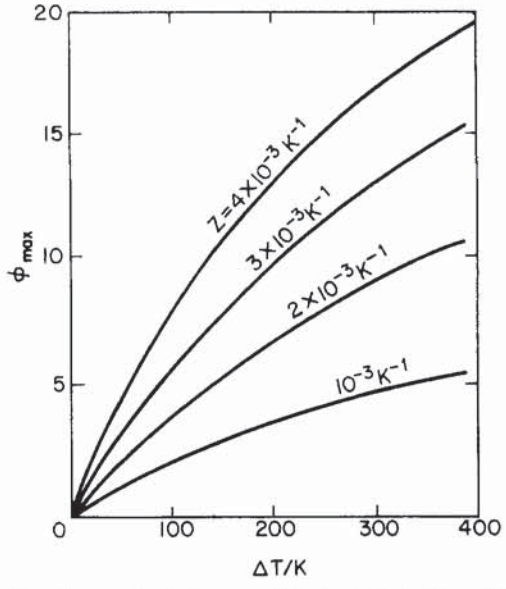

Fig. 5. Efficiency of a thermoelectric generator as a function of temperature for a cold junction temperature of 300 K.

A high efficiency device should have a large Z value and operate over as wide a temperature range as possible, fig. 5, but the value of Z depends upon the level of doping. The optimum doping level decreases with increase in temperature, until a stage is reached when minority carriers begin to be generated and it then rises again. Ideally, the arms of the thermocouple should have a 'doping gradient', but so far this has not been really tried. The emphasis has been on developing materials with a high value of Z over a relatively narrow temperature range and then relying on device technology to extend the working temperature range. An approximation to the 'graded thermocouple' is the sandwich arrangement of fig. 6. Here, each section operates at its best average Z value and the overall figure of merit is given by the envelope of the individual figures of merit. The main disadvantage is the large number of contacts. For large temperature differences the idea can be extended using

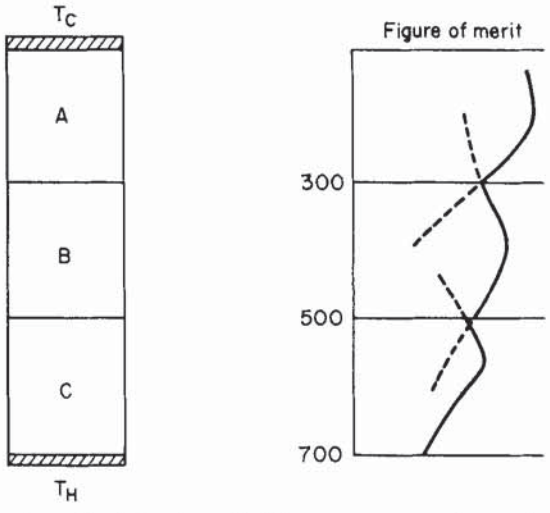

Fig. 6. Principle of sandwich arrangement of materials.

several different materials in a 'segmented' arrangement, fig. 7. The difficulties posed by the geometrical requirements of each segment for optimum performance, are partially overcome in the cascade arrangement, fig. 8, in which the different couples fabricated from different materials are thermally in series but electrically insulated from one another. The second stage of thermocouples uses heat rejected from the first stage and so on. In multistage devices, silicon–germanium is invariably employed at the high temperature stage(s) and an efficiency of 13% has been reported for a two-stage power generating thermocouple constructed from Si–Ge and $(Bi, Sb)_2$ $(Te, Se)_3$ alloys, (fig. 9, Rosi 1968). Heat sources consisting of radioactive isotopes of long half-life (Penn 1974) are used in radiosotopic thermoelectric generators (r.t.g.s).

At lower power levels the total cross-sectional area of thermoelectric material is relatively small in comparison with the surface area of the fuel source. Consequently an appreciable fraction of the available heat bypasses the thermoelements. The

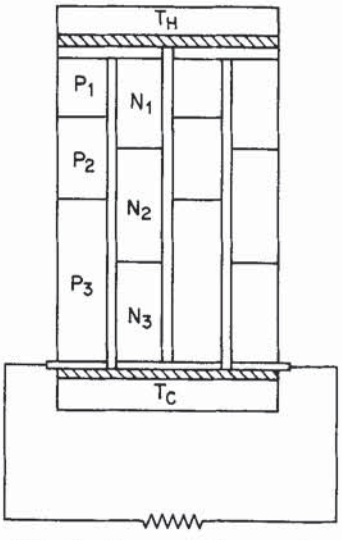

Fig. 7. Segmented generator.

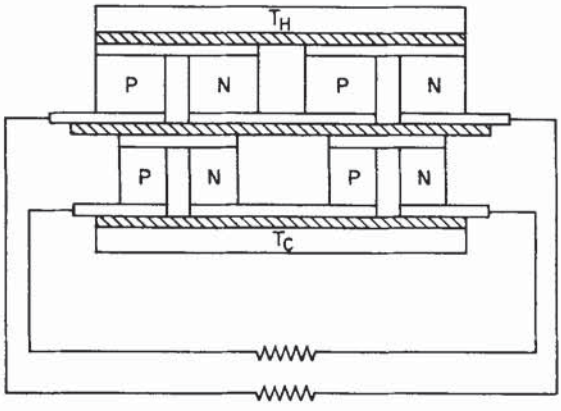

Fig. 8. Cascaded arrangement.

conversion efficiency of an r.t.g. depends upon the operating temperature and the relative proportions of the available heat that are transferred through the module and through the thermal insulation. At high power levels less heat bypasses the thermoelements so the efficiency of the device increases. Usually the cold-side temperature is fixed by the ambient temperature and so at each power level there is an optimum hot-side operating temperature which increases with increase in power.

In the low power range ($\sim 300\,\mu W$) bismuth telluride generators are the most efficient, followed by lead telluride, with silicon–germanium last. However the differences in the overall device efficiences at these power levels are marginal because one can make silicon–germanium thermocouples of high length : cross-section ratio. These thermocouples provide voltages which do not need any d.c.-to-d.c. converter (Raag 1971). Above 50 mW, silicon-germanium r.t.g.s give the best performance.

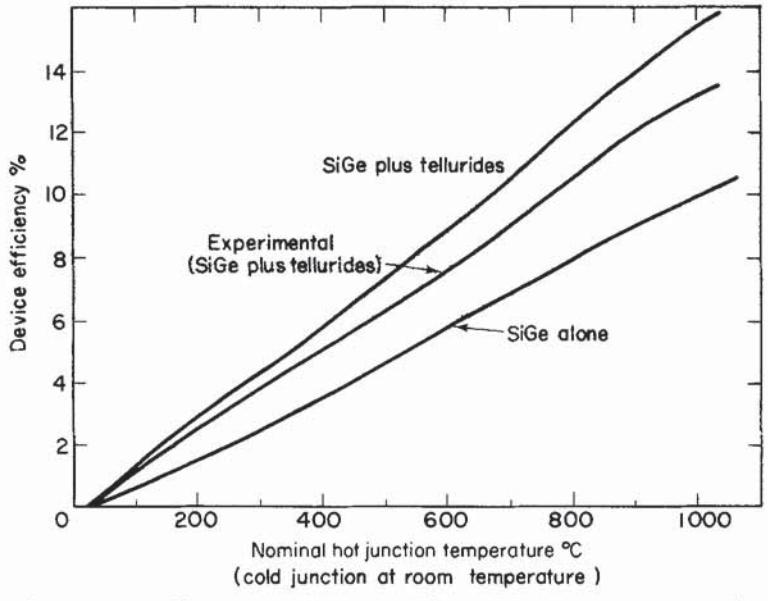

Fig. 9. Comparison of device and theoretical efficiencies versus temperature for a two stage power generating thermocouple constructed from Si–Ge and $(Bi,Sb)_2(Te,Se)_3$ alloys (After Rosi 1968).

As to the recently developed selenides, copper–silver selenide serves as the p-type and gadolinium metal the n-type material. The good thermoelectric properties are due to a disordered lattice structure and non-stoichiometric doping. Gadolinium metal with consistent properties is difficult to prepare, and information on these materials is scarce (Hampl *et al.* 1975). Nevertheless they are sufficiently promising to be chosen as the thermoelectric material for use in the 'low-cost, high-performance generator' (LCHPG) technology programme initiated by the U.S. Air Force in 1973 and are predicted to operate with an overall efficiency of 13·5% by 1985 (Lieberman 1976).

The configuration of the thermoelements in devices is determined to a large extent by the intended application. In space applications where cold junction temperatures are relatively high and one wants to encourage heat losses by radiation, the thermoelements are usually mounted individually and radially around the heat source. Thermoelectric generators based upon silicon–germanium are employed in the multi-hundred-watt r.t.g. developed for the American Air Force Communication Satellite launched in 1976 (Kelly 1975). Similar, multi-hundred-watt generators were used to power the Jupiter/Saturn Voyager Spacecraft illustrated below.

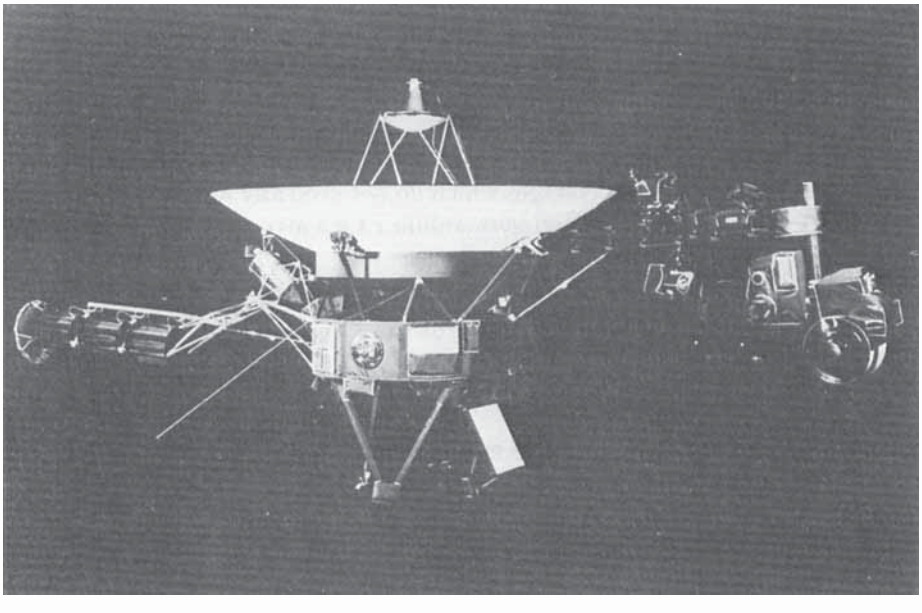

The Voyager spacecraft weighs 795 kg including 113 kg of scientific instruments. The Voyager 1 arrival dates for Jupiter, March 5, 1979, and for Saturn November 12, 1980. Voyager 2 arrival dates, July 9, 1979 for Jupiter and August 27, 1981 for Saturn. Voyager 2 may be targeted for Uranus flyby in January 1986. The large antenna at top is 3·66 m in diameter. Struts at the bottom attach to the solid propellant propulsion module, which separates after giving the spacecraft its final push to Jupiter. A gold-plated copper record of Earth greetings, sights, and sounds is inside a gold-plated aluminium canister which has instruction symbols on its face, and is attached to one of the ten sides of the spacecraft (centre). On the boom at left are the nuclear power generators. Above this boom is the 13 m extendable magnetometer boom in its aluminium canister. On the end of the science boom at the right is a steerable platform for optical instruments. (Courtesy of NASA and the Jet Propulsion Laboratory, California Institute of Technology.)

4. Silicon–germanium alloy preparation

Silicon and germanium both have the diamond structure, and with similar lattice constants, of 0·5431 nm and 0·5657 nm respectively, are able to form a continuous series of solid solutions. Undoped alloys of the required composition can be prepared by heating the component elements in a crucible or by the thermal decomposition of $GeCl_4$ and $SiHCl_3$ (though the latter method does not in fact give the high carrier concentrations required in thermoelectric applications).

The electronic configuration of silicon–germanium is such that the addition of suitable amounts of Group 3B elements render it p-type, while those of Group 5B render it n-type. Boron gives carrier concentrations in excess of $10^{26}\,m^{-3}$ quite easily, if added directly into the alloy melt. The addition of Group 5B dopants such as arsenic or phosphorus, which have suitable high solubilities, particularly in silicon-rich alloys requires rather more elaborate techniques and their high toxic and volatile nature requires completely enclosed systems, the dopant usually being in the vapour phase.

Although silicon and germanium form a continuous solid solution, the phase diagram with its wide separation of liquidus and solidus is unfavourable and it is difficult to produce homogeneous alloy crystals. On cooling from a silicon–germanium alloy melt, silicon-rich crystals are deposited after reaching the liquidus curve. With further cooling the composition of the crystals and that of the melt change according to the respective solidus and liquidus curves. The alloy formed is usually inhomogeneous and is not readily improved by annealing.

Although they are not essential for thermoelectric device applications homogeneous materials of constant composition are indeed needed if the effect is to be studied properly, and homogeneous alloy specimens of constant composition can be prepared by isothermal solidification, from a melt of constant composition.

Recently there has been more interest in hot pressing techniques as at the high doping levels used, the material is less affected by contamination.

The regular and repetitive production of alloys which have the same mechanical and electrical properties, is quite a difficult although essentially practical problem. Coarse powder reduces the density of the pressing, while very fine powder results in a molten phase, so the average particle size of the hot pressed powder is fairly critical.

Although the molten phase is known to be germanium-rich, its origin is uncertain. Lefever *et al.* (1974) suggested that as the starting powder is chemically inhomogeneous and as germanium-rich alloy pulverizes more readily than silicon-rich material, the melting may be the result of finely divided germanium-rich powder dispersed between coarser particles of silicon-rich powder. Temperature and pressure are also critical.

The beneficial results of hot pressing are often offset by some degradation in electrical properties, particularly in carrier mobility. In 99·6% dense alloy the carrier mobility is 5% lower than that in single crystal material. The presence of oxygen, both dissolved and absorbed on the interparticle surfaces may be partially responsible. At vacuum better than $0{\cdot}1\,Nm^{-2}$ silicon surfaces can be thermally regenerated. Adsorbed layers on germanium may be removed by heating to 900 K in high vacuum. In addition oxygen is likely to interact with the usual dopants in silicon–germanium alloys, such as phosphorus and boron, and may be responsible for some degradation of the electrical properties. To ensure a very low oxygen content, the hot presses can be operated in vacuum.

5. Thermoelectric figure of merit—general theoretical considerations

Elementary considerations show that thermoelectric materials should possess a large Seebeck coefficient to generate a large voltage, with a low electrical resistivity to minimize Joule heating and a low thermal conductivity to minimize heat losses from the thermocouple junctions.

Rittner (1959) discussed the case of a thermocouple with n- and p-type branches of the same material. He considered a rather simplified model and assumed that conduction takes place in a single band, that the mean free path varies as the rth power of the carrier energy and the lattice component of the thermal conductivity is negligible compared to its electronic component.

In a single-band model the Fermi level may diverge indefinitely from the band edge and lead to unrealistically large values of the Seebeck coefficient. This difficulty was avoided by restricting the Fermi level to its intrinsic value which is really equivalent to assuming the existence of a second band. The maximum value of the figure of merit is given by

$$Z_{\max} = (r+2+\Delta E/2kT)/(r+2)T,$$

ΔE being the intrinsic energy gap. This expression gives a value for the figure of merit which is an order of magnitude higher than has so far been observed in any material.

Littman and Davidson (1961) concluded from arguments based on thermodynamics that the second law does not impose any upper limit on Z. However this does not necessarily mean that it is possible to increase Z indefinitely. And we should be guided by the specific model of the solid being considered and the extent to which this may be realized in practice.

Simon (1962) investigated a general two-band semiconductor model treating each branch of the couple separately. Rittner and Neumark (1963) used this model to discuss the question of a finite upper bound to the figure of merit and the factors which favour a high value of this upper bound. They concluded that a high upper bound could be obtained subject to a large ratio for effective masses of holes and electrons, m_h/m_e along with a small absolute value of m_e.

In almost all theoretical models a contradictory condition appears in that the lattice component of heat conduction should be as small as possible and the energy band gap as large as possible. Some other requirements are: the acoustic phonon scattering of carriers should predominate in the negative branch of the couple and impurity scattering in the positive branch. Further it is desirable to have a large number of equivalent extrema in the conduction band. A large mass anisotropy is desirable for electrons but not for holes.

5.1. *Thermoelectric figure of merit of silicon–germanium alloys*

The thermoelectric figure of merit (Z) depends upon the electrical and thermal conductivities and the Seebeck coefficient.

In obtaining the theoretical value of (ZT) an approach similar to that followed by Ure (1972) seems the most realistic, although as he remarks "Parameters concerned with charge carriers (mobility, electrical conductivity) come mainly from III-V compounds and Si and Ge while the parameters for thermal conductivity come from a different set of materials." He shows that an increase of 10 to 20% in ZT seems a reasonable aim, although an increase by a factor of 2 is very unlikely.

In principle, the figure of merit could be obtained from the experimental measurements of the thermal and electrical conductivity and the Seebeck coefficient. All three properties vary with carrier concentration and it is convenient to express the thermoelectric figure of merit in terms of a single variable, the reduced Fermi energy ξ which depends upon the level of doping, together with a number of constant parameters.

Dismukes *et al.* (1964) presented a detailed investigation of thermal and electrical properties of these alloys as a function of composition, doping concentration and temperature. The requirements of a large energy gap to minimize intrinsic conduction at high temperature and that of a high melting point favours silicon rich alloys. Consequently, the most extensively investigated alloys were of $Si_{0\cdot70}Ge_{0\cdot30}$, $Si_{0\cdot80}Ge_{0\cdot20}$ and $Si_{0\cdot85}Ge_{0\cdot15}$ compositions.

5.2. *Thermal conductivity*

Measurements of thermal conductivity of single crystals of Si–Ge alloys as a function of temperature, composition and doping concentration have been reported by Dismukes *et al.* (1964) and Erofeev *et al.* (1966). These results are in agreement with each other although a quantitative theoretical explanation of the variation of thermal conductivity with doping concentration has been somewhat uncertain (Steigmeier 1969).

Thermal resistivity changes significantly with alloy composition due to atomic disorder scattering, as shown in fig. 10. Separate curves show the case of undoped alloy and of the alloy doped with boron, arsenic and phosphorus. For a particular curve the rise in thermal resistivity is attributed to the scattering of phonons by point defects while the difference between two curves is possibly due mainly to the scattering of phonons by free charge carriers (Rosi 1968, Steigmeier and Abeles 1964, Steigmeier 1969).

The disorder produced by alloying has two important effects:

(*a*) It increases thermal resistivity by scattering phonons according to a fourth-power-of the-frequency law (Carruthers 1961, Drabble and Goldsmid 1961).

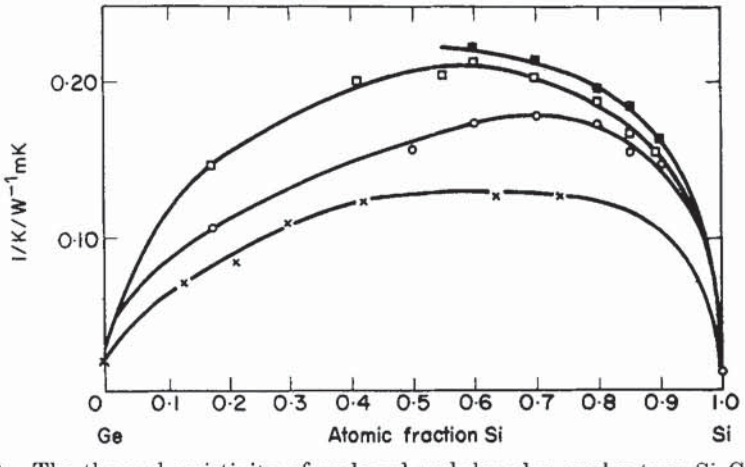

Fig. 10. The thermal resistivity of undoped and doped p- and n-type Si–Ge alloys as a function of alloy composition at 300 K. (After Dismukes *et al.* 1964) ×, undoped; 0, $1\cdot5 \times 10^{26}$ m^{-3} p-type B: □, $1\cdot5 \times 10^{26}$ m^{-3} n-type As; ■, $1\cdot5 \times 10^{26}$ m^{-3} n-type P.

(*b*) It scatters the high frequency phonons more effectively which makes boundary scattering appreciable even at normal temperatures (Goldsmid and Penn 1968). This point is discussed in more detail in the following paragraphs.

The effect of scattering due to charge carriers is shown in figs. 11(*a*) and (*b*) where the thermal resistivity of p and n-type alloys is displayed as a function of temperature and carrier concentration, and the effect of doping on thermal conductivity is obvious from the figure. An explanation of this reduction was given by Steigmeier and Abeles (1964) in terms of an additional scattering of phonons by charge carriers using Ziman's (1956) expression for the relaxation times. Figure 12 indicates the relative significance of various scattering processes in limiting the mean free path of phonons.

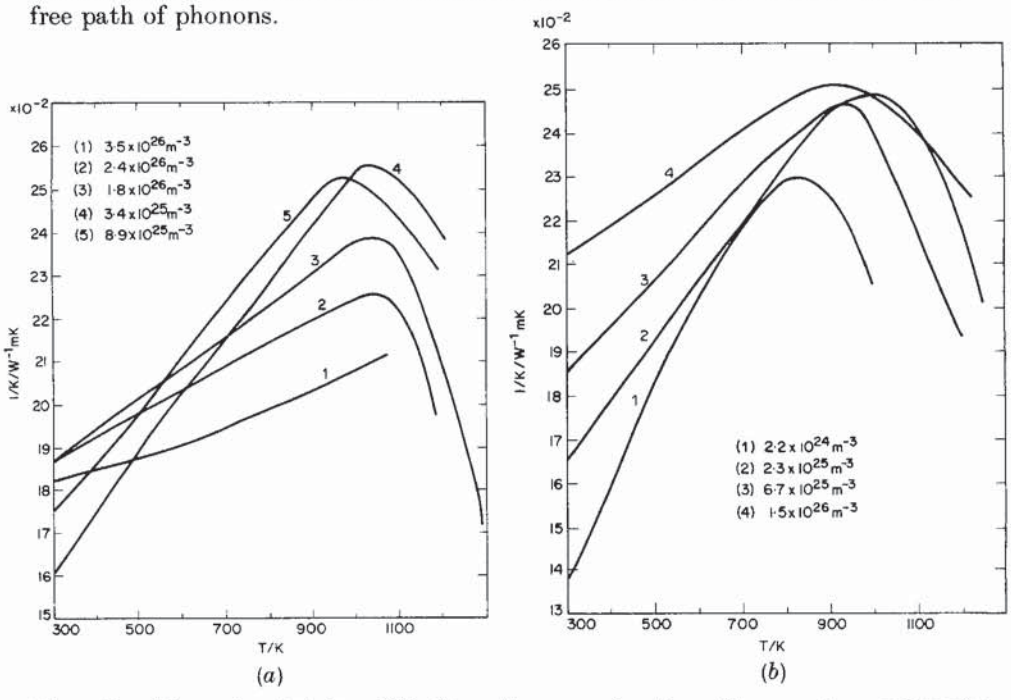

Fig. 11. Thermal resistivity of $Si_{70}Ge_{30}$ alloys as a function of temperature and carrier concentration. (*a*) p-type; (*b*) n-type. (After Dismukes *et al.* 1968.)

Erofeev *et al.* (1966) attributed the reduction in thermal conductivity by doping to the scattering of phonons by strains produced by ionized impurities instead of scattering by carriers. Their argument relied on the absence of any observed effect of phonon drag on the thermoelectric power. However, Steigmeier (1969) criticized the interpretation on the grounds that whereas the electron–phonon interaction is important in the scattering of phonons it is not the predominant scattering mechanism for electrons.

Goldsmid and Penn (1968) pointed out that boundaries may scatter phonons effectively at high temperature if the high frequency phonons can be scattered effectively by disorder in the lattice. The heat is then carried primarily by the low frequency phonons which are particularly sensitive to boundary scattering. Thus, although the mean free path of the phonons is decreased by the formation of a solid solution, this actually makes boundary scattering much more effective. Figure 13

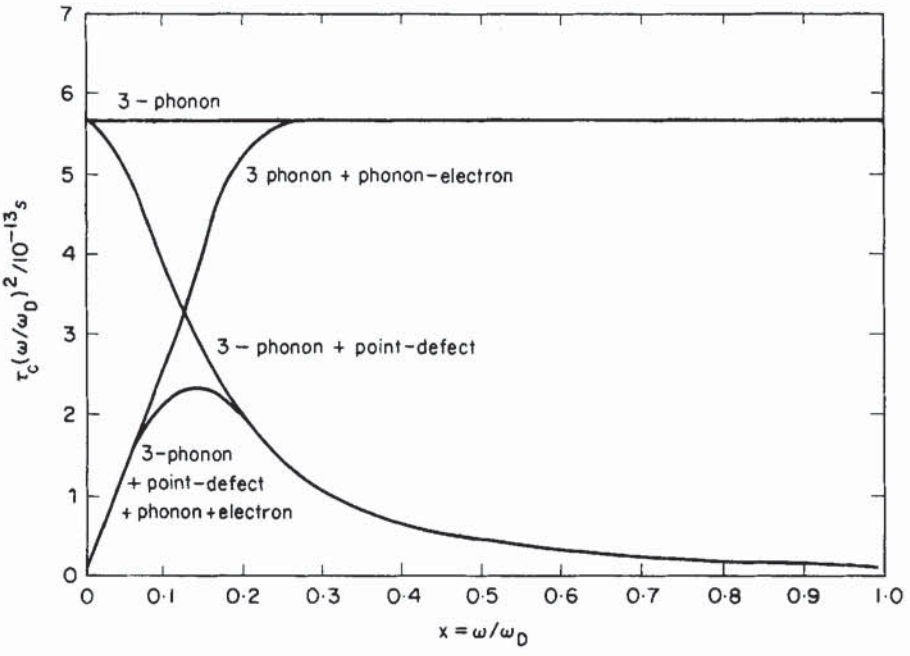

Fig. 12 The quantity $\tau_c x^2$, which determines the lattice thermal conductivity, as a function of reduced phonon frequency ω/ω_D for 3-phonon, point-defect and boundary scattering and their combinations. (After Steigmeier and Abeles 1964).

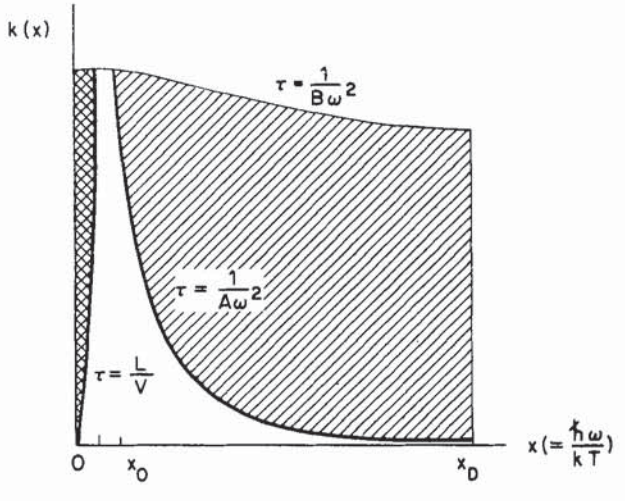

Fig. 13. Schematic plot of thermal conductivity against reduced phonon frequency $x = \hbar\omega/kT$. The processes considered are 3-phonon Umklapp processes ($\tau_n = 1/B\omega^2$), point-defect scattering and boundary scattering. Single-hatched area represents the reduction in thermal conductivity due to point-defect scattering. The double-hatched area indicates the reduction due to boundary scattering. (After Goldsmid and Penn 1968).

is a schematic plot of thermal conductivity against reduced phonon frequency $x=(\hbar\omega/kT)$.

The effect of hot pressing on the thermal resistivity, as compared with single crystals of the same material, has been estimated on the basis of a simple theoretical model (Parrott 1969) which predicted a 9% increase in a $Si_{70}Ge_{30}$ alloy with particle size 40 μm, though a somewhat different value has been obtained for thin films of neutron-irradiated silicon (Savvides and Goldsmid 1973). The thermal resistivity of very heavily doped alloys of Si–Ge was discussed by Meddins and Parrott (1976) and Bhandari and Rowe (1978), and a model calculation based on phonon dispersion relations was used for the variation of lattice thermal conductivity with grain size in n- and p-type alloys (Bhandari and Rowe 1978). These theoretical models gave satisfactory explanations of the observation that the thermal conductivity of thin films of silicon is lower than that of the bulk, single crystal material—although this explanation was not so satisfactory for sintered materials, particularly for heavily doped ones. Though even then, the possible extent of the reductions in thermal conductivity could be estimated and its influence on the thermoelectric figure of merit assessed. Figure 14 gives a plot of k_L against grain size for various doping concentrations. The combined effect of doping and alloying decreases the thermal conductivity in Si–Ge alloys to as low as $4\,W\,m^{-1}\,K^{-1}$ at 900 K and for material with a grain size of 0·1 μm it could go down to $2{\cdot}5\,Wm^{-1}\,K^{-1}$ where it becomes almost independent of carrier concentration (Bhandari and Rowe 1978). The variation of the lattice thermal conductivity (k_L) with energy gap (E_g) in Si–Ge alloy systems is shown in fig. 15.

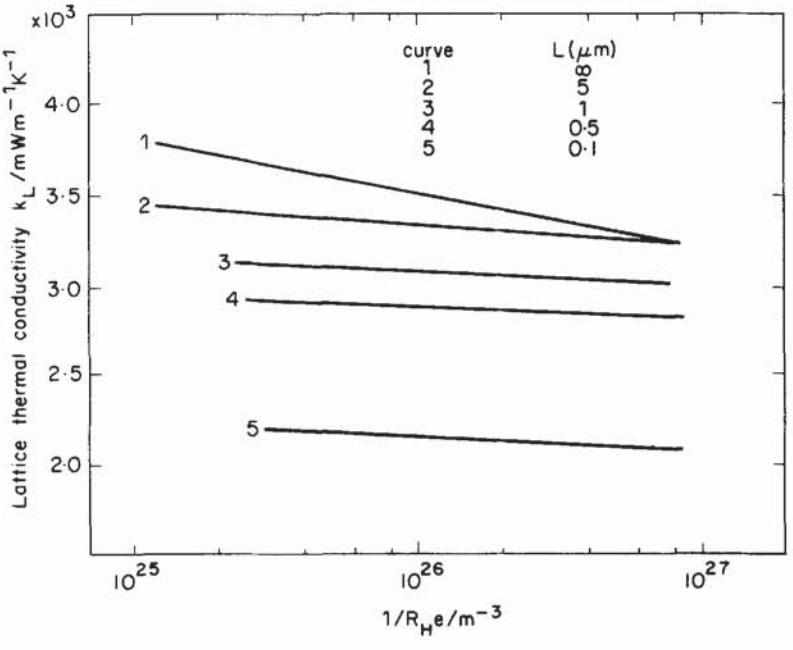

Fig. 14. k_L versus grain size and carrier concentration in p-type $Ge_{0\cdot30}\,Si_{0\cdot70}$ alloy at 900 K (Theoretical, after Bhandari and Rowe 1978a).

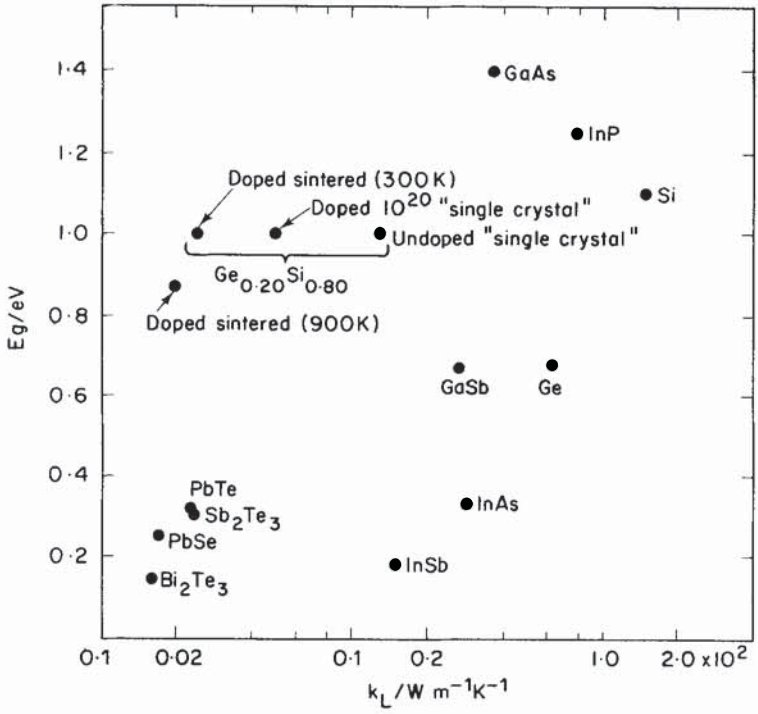

Fig. 15. Lattice thermal conductivity and energy gap of Ge–Si system, along with those of other important semiconductors. Values correspond to room temperature unless stated otherwise. Sintered material corresponds to a grain size of 0·1 μm. (After Bhandari and Rowe 1978).

5.3. *Electrical properties*

The electrical properties of single crystal silicon–germanium alloys were measured by Dismukes *et al.* (1964) over a wide range of temperatures (300–1300 K) and carrier concentrations (2×10^{24}–4×10^{26} m^{-3}). The silicon content of the alloys varied from 67% to about 87%. For p-type alloys the electrical resistivity and Seebeck coefficient were found to increase nearly linearly with temperature. The Hall mobility was found to vary approximately as $T^{-0.8}$. The mobility in heavily doped alloys is considerably smaller than in the lightly doped alloys, due to additional scattering of carriers by ionized impurities. Earlier measurements of mobility in germanium-rich alloys were reported and analysed on the basis of the theory of Nordheim and Brooks (Glicksman 1958, Levitas 1955).

At room temperature the conduction band minima are of L_1 type ((111) minima, as in Ge) for (0–10) atomic percentage of silicon and of the Δ_i type ((100) minima as in Si) for 20–100 atomic percentage of Si. For the intermediate range (10–20 atomic percentage of Si) both conduction bands are populated and contribute to conduction.

The variation of the electrical resistivity of p-type Si–Ge alloys with temperature and carrier concentration is shown in fig. 16. In some alloys electrical resistivity rises with temperature, reaches a maximum and then starts decreasing. This is observed in alloys with low carrier concentration, and is due to the onset of intrinsic conduction. In materials with high carrier concentration this maximum is expected to occur at higher temperatures.

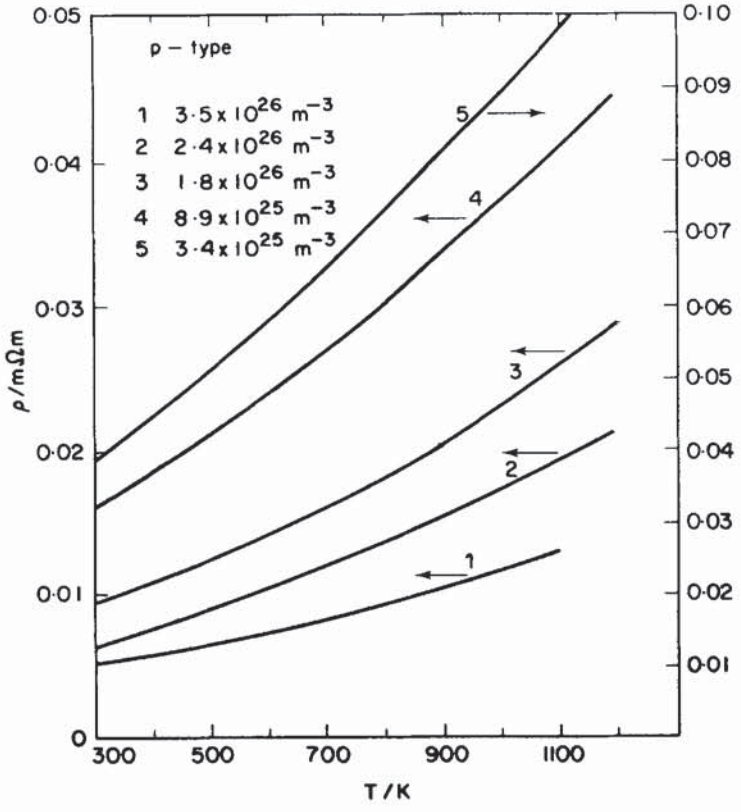

Fig. 16. The electrical resistivity of p-type $Si_{70}Ge_{30}$ alloys as a function of temperature. (After Dismukes *et al.* 1964).

The variation of the Seebeck coefficient and electrical resistivity with the charge carrier concentration is important in the theory of thermoelectricity. There should, according to the theory, be an optimum doping level (expressed as the optimum value of Fermi potential) in the range 10^{24}–$10^{26}\,m^{-3}$—although the figure of merit values obtained from measurements of the Seebeck coefficient and the electrical and thermal conductivities suggest that the figure of merit should have its maximum value at carrier concentrations greater than $10^{26}\,m^{-3}$. (Dismukes *et al.* 1964, Meddins and Parrott 1976).

Amith (1964) investigated the carrier scattering by assuming, in $Si_{0\cdot70}Ge_{0\cdot30}$ alloys, two separate relaxation times due to scattering, one by acoustic phonons and alloy disorder, and the other by ionized impurities. The Hall coefficient R_H, the Seebeck coefficient and the electrical resistivity depend on the reduced Fermi energy and on the carrier scattering, so both of them can be found from a set of measurements on a single sample.

Electrical conductivity measurements made on hot-pressed alloys indicate that a grain of size about 10 μm is almost ineffective in scattering charge carriers. This could be expected as their mean free path is considerably less than the grain size (Rowe 1975, Meddins and Parrott 1976). Room temperature measurements of electrical resistivity, Hall mobility and Seebeck coefficient (Rowe 1975) on p-type alloys show that the Seebeck coefficient as a function of $1/R_He$ is more or less indistinguishable from corresponding single crystal values (fig. 17). It has been shown (Suzuki and

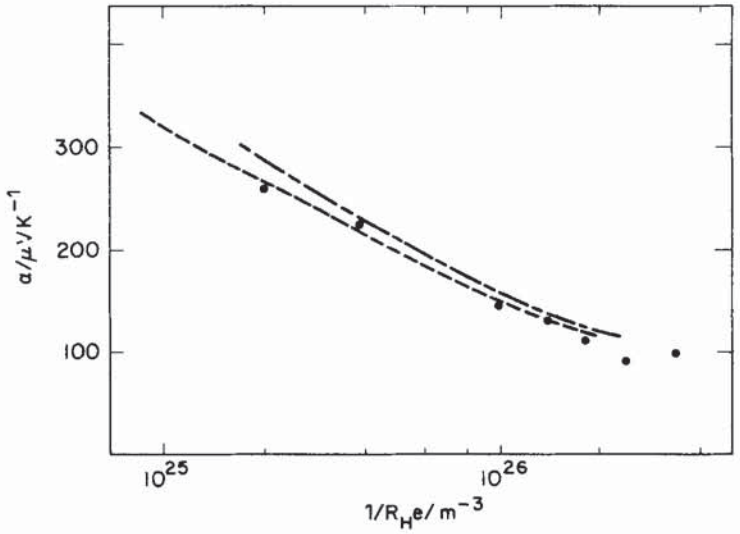

Fig. 17. Absolute Seebeck coefficient against $1/R_H e$ at room temperature for p-type Si–Ge alloy (after Rowe 1975). ●, UWIST hot-pressed; ——, Sandia high-density; ——·——·—— RCA sone-levelled.

Maki 1977) that in thin films of germanium the carrier mean free path may remain unaffected by boundary scattering down to film thickness of 1000 Å. On the basis of these results it is reasonable to assume that hot-pressing could add extra thermal resistance without significantly degrading the electrical behaviour. This tempts one to consider the case of hot-pressed alloys even if the degradation compensates for the increased thermal resistance thus rendering the figure of merit comparable to single crystal values solely on grounds of economy.

However, in the following we shall discuss an idealized model of hot-pressed Si–Ge alloy where electrical behaviour is assumed to remain unchanged down to 0·1 μm grain size. We call it the 'model HP alloy'.

The electrical behaviour can in principle, be analysed in terms of a single spherical valley model or the many-valley model provided sufficient information could be made available regarding the scattering of charge carriers. It is extremely difficult to give a quantitative picture taking all scattering mechanisms into account in a single calculation. However, figures of merit can be separately calculated for each individual mechanism. The following scattering mechanisms are effective in limiting the carrier mean free path in n-type Si–Ge alloys.

Intravalley scattering of carriers by acoustic phonons.
Intervalley scattering
Optical mode scattering
Ionized impurity scattering
Scattering by alloy disorder.

The electrical conductivity can be expressed in a form convenient for computation. One assumes a carrier relaxation time of the form

$$\tau(E) = aE^S.$$

The so-called scattering parameter S takes different values for different scattering mechanisms. The carrier mobility in terms of the relaxation time can be

written as

$$\mu = \frac{e}{m_c}\langle\tau\rangle.$$

Here m_c is the conductivity (inertial) effective mass and $\langle\tau\rangle$ is the average relaxation time.

The reduced electrical conductivity takes the form

$$\sigma = \frac{A'F(s+\frac{1}{2})(\xi)}{(s+\frac{1}{2})!}$$

Where $F_n(\xi)$ is a Fermi integral of order n

and

$$A' = \frac{2(2\pi k)^{3/2}k^2A''}{eh^3}$$

$$A'' = T^{5/2}(m^*)^{3/2}\mu/k_L$$

$m*$ is the density-of-states effective mass. The mobility itself depends upon the effective mass and this dependence will vary with the particular scattering mechanism considered. For scattering by acoustic phonons

$$\mu_{ac} = \frac{(8\pi)^{1/2}e\hbar^4C_{11}}{3(kT)^{3/2}(m^*)^{5/2}\varepsilon_1^2}$$

and hence

$$A'' = \frac{(8\pi)^{1/2}e\hbar^4}{3k^{3/2}}\frac{C_{11}T}{m^*\varepsilon_1^2k_L}.$$

C_{11} is an elastic constant and ε_1 is the acoustic deformation potential constant.

It is important to distinguish between an inertial (conductivity) mass m_c and density-of-states mass m^*. For a single spherical valley case

$$\mu_{ac} \alpha m_c^{-1}(m^*)^{-3/2}.$$

And A'' is inversely proportional to m_c. For a many-valley model, ignoring intervalley scattering,

$$\mu_{ac} \alpha N m_c^{-1}(m^*)^{-3/2}$$

where N is the number of valleys. This relation implies that mobility depends on the inertial mass m_c and also on a density-of-states mass for a single valley which is $N^{-2/3}$ times the overall density-of-states mass m^*. This leads to (Goldsmid *et al.* 1958)

$$A''\alpha N/m_c.$$

It appears from this that a multivalley structure would favour a higher figure of merit. However, intervalley scattering would be significant and may reduce mobility depending upon the strength of scattering.

Although there are detailed discussions of intervalley scattering in n-type silicon (Long 1960, Dumke 1960) there is not sufficient information on the strength and nature of this mechanism in Si–Ge alloys. Moreover there are discrepancies even in the case of silicon (Long 1960). However as the band structure of these alloys is similar to silicon an approximate description of the situation in n-type Si–Ge alloy can be attempted.

This introduces three new parameters, Θ_i a phonon characteristic temperature; W_1 representing the strength of acoustic scattering within a potential valley (intravalley scattering); and W_2 representing the strength of acoustic scattering between potential valleys (intervalley scattering).

It has been mentioned (Seeger 1973) that in n-type silicon the temperature dependence of mobility can be described by an analysis similar to that of Herring (1955).

The combined effect of the two scattering mechanisms on carrier mobility are described (Seeger 1973) by the equations:

$$\mu/\mu_0 = f(T/\Theta_i) \text{ and } \mu_0 = \mu_{ac}(T/\Theta_i)^{3/2}$$

Choosing $\Theta_i = 720$ K and $W_2/W_1 = 2{\cdot}0$ the figure of merit in n-type Si–Ge alloys has been obtained in terms of the reduced Fermi energy (fig. 18). The closest fit to the results of Dismukes *et al.* (fig. 19) is obtained using curves III and IV. Curves I and II give ZT values which are substantially less than those observed experimentally.

At 1000 K the dominant scattering mechanism is the intervalley scattering while at 300 K the ionized impurity scattering is significant in heavily doped alloys.

The mobility ratios μ_{ac}/μ_{ii} and μ_{ac}/μ_{dis} indicates the relative strengths of ionized-impurity and alloy disorder scattering at 300 and 1000 K respectively as indicated in the table (Bhandari and Rowe, unpublished).

It is useful to compare these results with those obtained from experimentally measured values of electrical and thermal conductivities and of the Seebeck coefficient (Dismukes *et al.* 1964, Rosi 1968 and fig. 19).

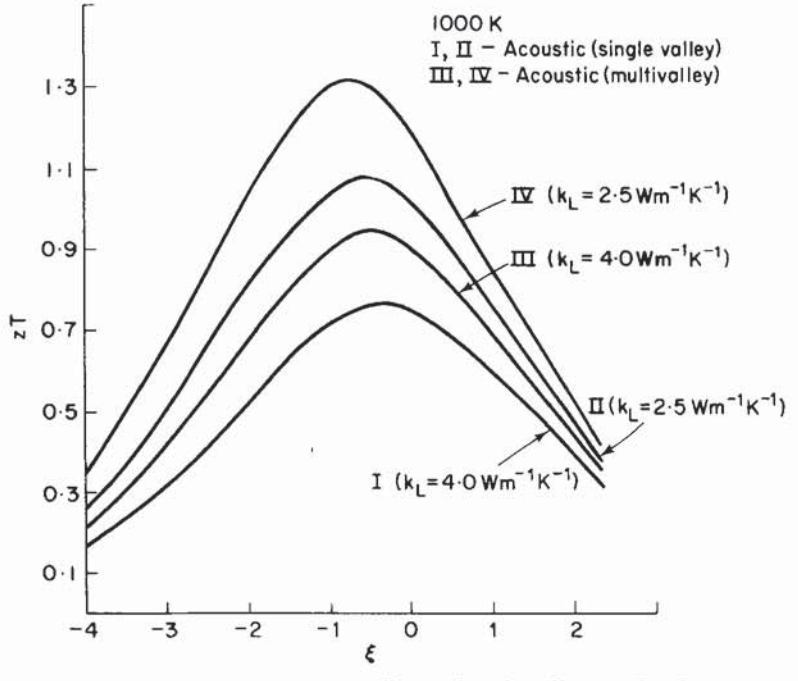

Fig. 18. ZT against ξ at 1000 K. Single valley and multivalley results shown separately for two different k_L values. The multivalley calculations take account of intervalley scattering with $w_2/w_1 = 2{\cdot}0$ and $\Theta_i = 720$ K. $E_1 = 10$ eV, $m^*/m_0 = 0{\cdot}29$; $\xi_g = 10$, is the reduced energy gap, (Bhandari and Rowe unpublished) curves II and IV refer to the model H P alloy.

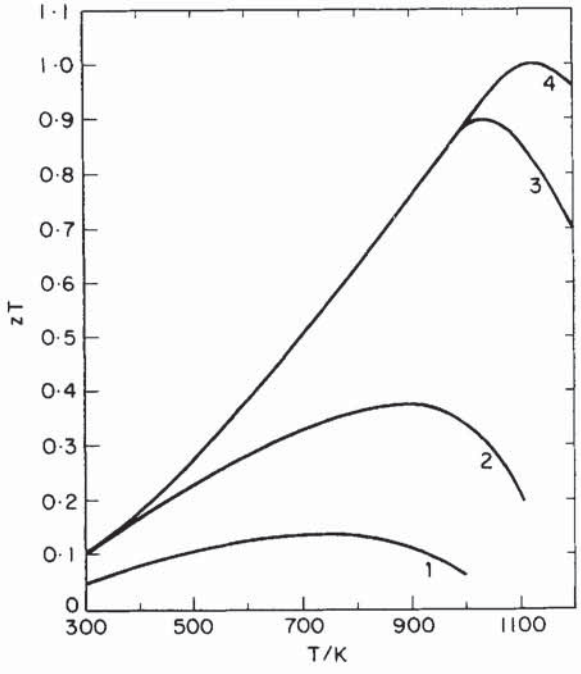

Fig. 19. The dimensionless figure of merit ZT of n-type $Si_{70}Ge_{30}$ alloys as a function of temperature. Carrier concentrations (1) $2{\cdot}2\times10^{24}\,m^{-3}$ (2) $2{\cdot}3\times10^{25}\,m^{-3}$ (3) $6{\cdot}7\times10^{25}\,m^{-3}$ (4) $1{\cdot}5\times10^{26}\,m^{-3}$ respectively (After Dismukes *et al.* 1964).

Their results indicate that an optimum figure of merit and also a higher useful operating temperature of operation are found for very heavily doped material with carrier concentration greater than $10^{26}\,m^{-3}$, though theory gives optima at somewhat lower concentrations. The figure of merit versus temperature curves show broad maxima at high temperatures with average values of Z of about $0{\cdot}8\times10^{-3}\,K^{-1}$ and $0{\cdot}6\times10^{-3}\,K^{-1}$ for the n- and p-type alloys over the temperature range 700 to 1200 K (Rosi 1968).

Relative strengths of ionized-impurity and alloy disorder scattering at 300 and 1000 K

T/K	$\mu^{\dagger}_{ac}/\mu^{\ddagger}_{ii}$	$\mu^{\dagger}_{ac}/\mu_{dis}$
300	8	0·28
1000	0·26	0·04

† Includes the effect of multivalley structure including intervalley scattering.

‡ The mobility refers to the alloy with reduced Fermi level $\xi\cong0$ (corresponding to optimum doping).

5.4. *Material instability*

Silicon–germanium alloys are used in power sources covering the range 150 μW to 150 W, working best at the upper temperature ranges. Most of the applications are meant to last more than ten years. Unfortunately the thermoelectric behaviour changes with time owing to dopant precipitation and sublimation of the material—the effects of which increase with increasing temperature.

The CalTech Jet Propulsion Laboratory (USA) has sponsored programmes for the investigation of the variation with time and with temperature of the thermoelectric properties of these alloys. Initially it had been assumed that the solubility of boron in Si–Ge was sufficiently high to preclude possible precipitation and attention was focused on phosphorus, the solubility of which for optimization of Z is marginal. Good agreement between experiment and theory has been obtained for n-type behaviour and work is now proceeding for p-type behaviour.

Early investigations were also confined to the variation with time of the electrical properties as it was believed that the thermal conductivity varied little with time. But recent results indicate that thermal conductivity does change with time. An explanation put forward by Raag is that the alloys at present in use are not true alloys, but rather mixtures of particles of widely varying compositions. The measured lattice thermal conductivity is really that of a series parallel combination of individual grains each of which has its own effective thermal conductivity. But actual alloying is enhanced as time goes on, and as temperatures rises. There is little information about changes in thermal conductivity with time and temperature, but what there is supports the view that the thermal conductivity should decrease with time.

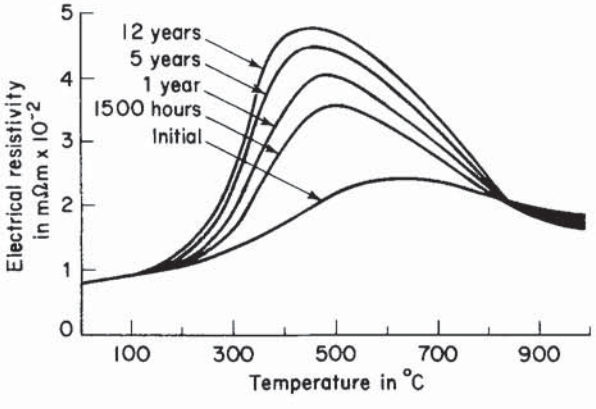

Fig. 20. Electrical resistivity of n-type $Si_{78}Ge_{22}$ alloy (after Raag 1976).

The time and temperature variation of the electrical resistivity of n-type $Si_{78}Ge_{22}$ alloys is shown in fig. 20. The time variation itself depends upon temperature, with the greatest time variation in electrical properties for n-type alloys appearing around 400 to 500°C. In p-type alloys the greatest time variation in electrical properties occurred between 700 and 900°C. The thermal conductivity does not vary with time below 600°C while above this the behaviour is somewhat different for n- and for p-type alloys. The results indicate a degradation of performance at high temperatures over a period of 12 years (fig. 21).

This degradation in performance is associated with the precipitation of the dopant from the solid solution. Let us consider the case of phosphorus as a dopant which has a marginal solubility in Si–Ge alloys for producing the maximum figure of merit. During the materials preparation the alloy is initially supersaturated with phosphorus. The precipitation of phosphorus out of the substitutional site changes

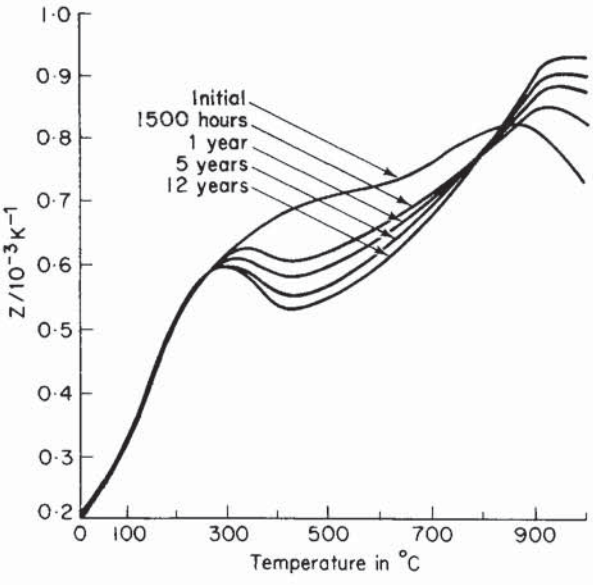

Fig. 21. Figure of merit of n-type $Si_{78}Ge_{22}$ alloy (after Raag 1976).

the electrical properties with time. Ekstrom and Dismukes (1966) have investigated the degradation in performance in these alloys using the theoretical model. Lifshitz and Slyozov (1961), Nasby and Burgess (1972) and Raag (1975) have suggested this approach to predict the long term behaviour.

The rate of precipitation is found to depend among other things on the nature of the dopant itself. The model of Lifshitz and Slyozov explains reasonably well the precipitation of phosphorus in these alloys. Boron also precipitates from the substitutional sites although the rate is much slower. On the basis of short term anneals it is possible to predict the long term behaviour of the material. Typical 'short term' anneals are of the order of 1500 to 6000 hours.

At the high temperatures for which they are used here, both germanium and silicon are appreciably volatile, with the vapour pressure of silicon about 1% that of germanium at the same temperature. Consequently they will sublime preferentially and deplete the surface. Eventually this results in a diffusion-limited system in which the materials come off in the rates in which they are incorporated in the alloy (Honig 1971). Attempts have been made to suppress sublimation by the use of a cover gas. Loss of material due to sublimation erodes the hot junctions and also decreases the cross-sectional area in its neighbourhood; both these effects increase the thermal resistance. Further, the evaporated material sublimes on to and between the insulation foils. This causes thermal losses through the material, which results both in loss of output power and decrease in the hot junction temperature. In addition the evaporated material will react with the fibrous insulation (SiO_2) which separates the foils from each other and from the hot source, adding to the interfoil deposits. Ultimately a shorting of the thermoelectric couples by the foils due to the complete loss of the fibrous material can result in a catastrophic failure of the generator.

The material losses cause erosion at the later stage. Investigations have shown that temperatures above 1050°C cannot be tolerated for a 12-year period (Stapfer and Truscello 1972).

7. Discussion and conclusion

The choice of thermoelectric material for a particular application is determined in the first instance by the intended temperatures of operation of the device. Silicon–germanium alloys can operate at substantially higher temperatures than any of the other established materials and its performance is comparable to its competitors when operating over the extremes of its operating temperature range.

Silicon–germanium thermoelements can be produced with extreme geometry which facilitates the production of low electrical power levels at relatively high voltages and reasonable conversion efficiency. Their capability to produce sufficiently large voltages for device operation without the need of a d.c.-to-d.c. convertor makes them especially attractive in miniature r.t.g. application. At all power levels thermoelectric generators based on silicon–germanium alloys are capable of higher direct output voltages than those employing the tellurides.

The predominant position of silicon–germanium alloys as high temperature materials appears to be strongly rivalled by the progressive improvement in the technology of the selenides, which have a high figure of merit and can operate at about 800°C. In space application when mass saving is a priority it is usually found that the lightest conversion system is obtained when the cold side of the thermoelectric generator operates around 300°C or higher. This restricts the choice of material to the selenides or silicon–germanium and although the selenides have been chosen by the American Air Force for their low-cost high-performance generators, silicon–germanium alloys are thought more suitable for solar thermoelectric generators (s.t.g.s) where near approaches to the Sun are envisaged (Raag 1978).

References

AMITH, A., 1964, *Proceedings of the Seventh International Conference on the Physics of Semiconductors* (Dunod), p. 393.

BATEMAN, P. J., 1960, *Contemp. phys.*, **2**, 302.

BHANDARI, C. M., and ROWE, D. M., 1978 a, *J. Phys.* C: *Solid St. Phys.*, **11**, 1787. 1978 b, *Proceedings of the Second International Conference on Thermoelectric Energy Conversion*, University of Texas at Arlington, March 1978 IEEE cat. No. 78 CH 1313-6 Reg 5, p. 32.

CARRUTHERS, P., 1961, *Rev. mod. Phys.*, **33**, 92.

DISMUKES, J. P., EKSTROM, L., STEIGMEIER, E. F., KUDMAN, J., and BEERS, D. S., 1964, *J. appl. Phys.*, **35**, 2899.

DRABBLE, J. R., and GOLDSMID, H. J., 1961, *Thermal Conduction in Semiconductors* (Pergamon Press), pp. 156–164.

DUMKE, W. P., 1960, *Phys. Rev.*, **118**, 938.

EKSTROM, L., and DISMUKES, J. P., 1966, *J. Phys. Chem. Solids.*, **27**, 857.

EROFEEV, R. S., IORDANISHVILI, E. K., and PETROV, A. V., 1966, *Soviet Phys. solid St.*, **7**, 2470.

GLICKSMAN, M., 1958, *Phys. Rev.* **111**, 125.

GOLDSMID, H. J., SHEARD, A. R., and WRIGHT, D. A., 1958, *Br. J. appl. Phys.*, **9**, 365.

GOLDSMID, H. J., and PENN, A. W., 1968, *Phys. Lett.* A, **27**, 523.

HAMPL, E. F., *et al.* 1975, *Proceedings of the Tenth Intersociety Energy Conversion Engineering Conference*, p. 714.

HERRING, C., 1955, *Bell Syst. tech. J.*, **34**, 237.

HONIG, R. F., 1971, *RCA Memo to distribution*, Harrison, N. J. 11 January.

KELLY, C. E., 1975, *Proceedings of the Tenth Intersociety Energy Conversion Engineering Conference*, p. 880.

LEFEVER, R. A., MCVAY, G. L., BAUGHMAN, R. J., 1974, *Mater. Res. Bull.*, **9**, 865.

LEVITAS, A., 1955, *Phys. Rev.*, **99**, 1810.

LIEBERMAN, A. R., *et al.* 1976, *Proceedings of the Eleventh Intersociety Energy Conversion Engineering Conference*, p. 1591.

LIFSHITZ, J. M., and SLYOZOV, V. V., 1961, *J. Phys. Chem. Solids*, **19**, 35.

LITTMAN, H., and DAVIDSON, B., 1961, *J. appl. Phys.* 32, **2,** 217.
LONG, D., 1960, *Phys.*, **120,** 2024.
MADANI, N., and ROWE, D. M., 1977. (Unpublished).
MEDDINS, H. R., and PARROTT, J. E., 1976, *J. Phys.* C: *Solid St. Phys.*, **9,** 1263.
NASBY, R. D., and BURGESS, E. L., 1972, *Proceedings of the Seventh Intersociety Energy Conversion Engineering Conference*, p. 130.
PARROTT, J. E., 1969, *J. Phys.* C: *Solid St. Phys.*, **2,** 147.
PENN, A., 1974, *Phys. Technol* **5,** 115.
RAAG, V., 1971, *Proceedings of the Sixth Intersociety Energy Conversion Engineering Conference*, p. 245.
RAAG, V., 1972, *Proceedings of the Seventh Intersociety Energy Conversion Engineering Conference*, p. 168.
RAAG, V., 1975, *Proceedings of the Tenth Intersociety Energy Conversion Engineering Conference*, p. 156.
RAAG, V., 1978, *Second International Conference on Thermoelectric Energy Conversion*, p. 5.
RITTNER, E. S., 1959, *J. appl. Phys.*, **30,** 702.
RITTNER, E. S., and NEUMARK, G. E., 1963, *J. applied Phys.*, **34,** 2071.
ROSI, F. D., 1968, *Solid-St. Electron.*, **11,** 833.
ROWE, D. M., 1975, *J. Phys.* D: *Appl. Phys.*, **8,** 1092.
SAVVIDES, N., and GOLDSMID, H. J., 1973, *J. Phys.* C: *Solid St. Phys.*, **6,** 1701.
SEEGER, K., 1973, *Semiconductor Physics* (Springer-Verlag), p. 250.
SIMON, R., 1962, *J. appl. Phys.*, **33,** 1830.
STAPFER, G., and TRUSCELLO, V., 1972, *Proceedings of the Seventh Intersociety Energy Conversion Engineering Conference*, p. 174.
STEIGMEIER, E. F., 1969, *Thermal Conductivity*, volume 2, edited by R. P. Tye (Academic Press), p. 299.
STEIGMEIER, E. F., and ABELES, B., 1964, *Phys. Rev.*, **136,** A1149.
SUZUKI, K., and MAKI, M., 1977, *Jap. J. appl. Phys.*, **16,** 667.
URE, R. W., JR., 1972, *Energy Convers.*, **12,** 45.
ZIMAN, J. M., 1956, *Can. J. Phys.*, **34,** 1256.